Large Notch Damage Evolution in Omega Stiffened Composite Panels

Available online at www.sciencedirect.com

ScienceDirect

Procedia Engineering 167 (2016) 151 – 159

Procedia Engineering

www.elsevier.com/locate/procedia

Comitato Organizzatore del Convegno Internazionale DRaF 2016, c/o Dipartimento di Ing. Chimica, dei Materiali e della Prod.ne Ind.le

Large Notch Damage Evolution in Omega Stiffened Composite Panels

A. Riccio[a,*], A. Sellitto[a], S. Saputo[a], A. Russo[a], V. Antonucci[b], M.R. Ricciardi[b], M. Zarrelli[b], V. Lopresto[c]

[a]*Department of Industrial and Informatics Engineering, Second University of Naples, via Roma 29, Aversa (CE), Italy*
[b]*CNR-IPCB Institute for Composites, Polymers and Biomaterials, National Research Council of Italy, P.le E Fermi, Portici, NA, Italy*
[c]*Department of Material Engineering, University of Naples "FEDERICO II", Pl.e Tecchio, Naples, Italy*

Abstract

The aim of this work is the study of the influence of a large notch damage in a stiffened aeronautical panel. In particular, the damage onset and evolution due to a cut-out located in the bay of an omega stiffened composite panel subjected to a compressive load is investigated. Three different cut-outs are considered: parallel, normal, and 45° oriented respect to the load. The effects of such configurations are compared in terms of fibre and matrix failures, in order to better understand which configuration is the most sensitive to these type of damages.

Peer-review under responsibility of the Organizing Committee of DRaF2016

Keywords: PFA; Intra-laminar damage; Large notch damage; Composite material; Finite element model

1. Introduction

Composite materials are usually characterised by high stiffness/weight and strength/weight ratios, hence they are suitable for application in many industrial sectors where the weight reduction is of primary concern. However, composites have been demonstrated very sensitive to damage (usually characterised by complex and hardy predictable failure mechanisms) leading to over-conservative designs, far from a full realization of the promising economic benefits.

* Corresponding author. Tel.: +39 081 5010 407; fax: +39 081 5010 204.
*E-mail address:*aniello.riccio@unina2.it

Peer-review under responsibility of the Organizing Committee of DRaF2016
doi:10.1016/j.proeng.2016.11.682

A relevant number of numerical approached can be found in literature for the prediction of onset and the evolution of intra-laminar and inter-laminar damages [1,2]. Among these, the Ultimate Laminate Failure models adopt a Progressive Failure Approach (PFA) to evaluate the ultimate load of composite laminates [3-8].

From literature, it appears clear that the material degradation phase and the related definition of damaged element residual stiffness are among the most critical aspects of a Progressive Failure Analysis. These aspects are still under investigation especially for complex composite components, such as stiffened panels, with a pre-existent damage susceptible to propagation under service loading conditions.

In this paper, the large notch damage evolution in an omega stiffened composite panel subjected to a compressive load by means of a Progressive Failure Approach has been investigated. Three different configurations of the large notch damage have been considered with notch differently oriented with respect to the load direction. The effects of notch orientation on the mechanical behaviour of the panel have been assessed. The numerical results for all the three analysed configurations have been compared in terms of intra-laminar damage onset and evolution, in order to better understand which configuration is the most notch sensitive. In Section 2, the theoretical background for the intra-laminar damage model adopted in this paper is presented. In Section 3, the investigated panels have been introduced with geometrical and FE models detailed description. Finally, in Section 4 the numerical results obtained for all the investigated configuration are presented and compared.

2. Intra-laminar damage model

An intra-laminar damage model has been adopted in this paper in order to study the effects of the large notch orientation on stiffened composite panels compressive behaviour. In particular, the Hashin's failure criteria [9-11] implemented in the standard version of the FE code ABAQUS and shown in Table 1, allowing the evaluation fibre and matrix compressive and tensile failure modes, have been used. The progressive intra-laminar damage has been simulated by assuming as internal state variables the damage index d_i, representative of the material stiffness degradation for each failure mode i.

Table 1: Test Matrix

Fiber tension	$\hat{\sigma}_{11} > 0$	$F_{ft} = \left(\frac{\hat{\sigma}_{11}}{X_T}\right)^2 + \left(\frac{\hat{\sigma}_{12}}{S_L}\right)^2 = 1$
Fiber Compression	$\hat{\sigma}_{11} < 0$	$F_{fc} = \left(\frac{\hat{\sigma}_{11}}{X_C}\right)^2 = 1$
Matrix tension	$\hat{\sigma}_{22} \geq 0$	$F_{mt} = \left(\frac{\hat{\sigma}_{22}}{Y_T}\right)^2 + \left(\frac{\hat{\sigma}_{12}}{S_L}\right)^2 = 1$
Matrix compression	$\hat{\sigma}_{22} \leq 0$	$F_{mc} = \left(\frac{\hat{\sigma}_{22}}{2S_T}\right)^2 + \left[\left(\frac{Y_C}{2S_T}\right)^2 - 1\right] \cdot \frac{\hat{\sigma}_{22}}{Y_C} + \left(\frac{\hat{\sigma}_{12}}{S_L}\right)^2 = 1$

According to Table 1, $\hat{\sigma}_{11}$ and $\hat{\sigma}_{22}$ are respectively the stress in the fibre direction and normally to the fibre direction; X_T, X_C, Y_T, Y_C, S_L, and S_T are respectively the Fibre tensile, Fibre compressive, Matrix Tensile, Matrix compressive, Longitudinal, and Transversal strengths. F_{ft}, F_{fc}, F_{mt}, and F_{mc} are respectively the values representative of the Fibre tensile, Fibre compressive, Matrix Tensile, and Matrix compressive criteria: when one of such criteria is met, the corresponding damage is initiated.

The graphical representation of the constitutive relations, describing the damage onset and evolution, adopted for each failure mode is shown in Figure 1.

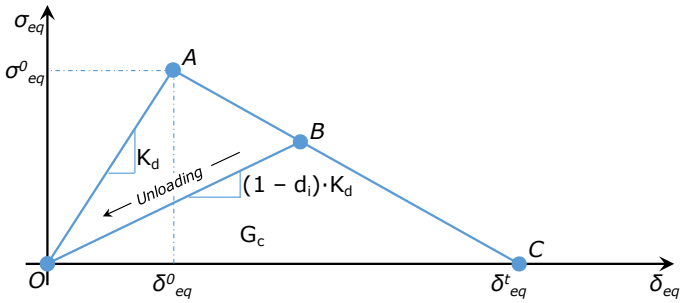

Figure 1: schematic representation of the constitutive relations adopted for each failure mode

Two different phases can be identified in the damage evolution: an initiation phase (segment OA) where the material is considered undamaged with a stiffness K_d and a degradation phase (segment OC) where damage starts and propagates. The point *A* in Figure 1 identifies the Hashin's stress limit value from which the degradation starts. Along the segment AC the degradation of the material properties occurs with a variation of the stiffness depending on the damage index d_i, according to the relation $(1 - d_i)\cdot K_d$. Finally point *B* represents a partially damaged condition and point *C* identifies the totally damaged condition.

The degradation damage coefficient d_i can assume values between zero (in the initiation phase) and one (in the totally damaged condition), and can be represented by the following relation:

$$d_i = \frac{\delta^t_{i,eq}\left(\delta_{i,eq} - \delta^0_{i,eq}\right)}{\delta_{i,eq}\left(\delta^t_{i,eq} - \delta^0_{i,eq}\right)}; \quad \delta^0_{i,eq} \le \delta_{i,eq} \le \delta^t_{i,eq}; \quad i \in \left(f_c, f_t, m_c, m_t\right) \tag{1}$$

where $\delta^0_{i,eq}$ and $\delta^t_{i,eq}$ are the equivalent displacements at which, respectively, the initiation criterion is met and the material is completely damaged ($d_i = 1$). Assuming a linear softening behavior, $\delta^t_{i,eq}$ can be calculated as:

$$\delta^t_{i,eq} = \frac{2G_c}{\sigma^0_{i,eq}} \tag{2}$$

where G_c is the fracture energy and $\sigma^0_{i,eq}$ is the equivalent stress that satisfies the failure criterion.

The equivalent displacements and stresses for each failure mode are reported in Table 2.

In Table 2, L_c is the element characteristic length, introduced to alleviate the mesh dependency effects during material softening, while < > is the Macauley bracket operator defined as:

$$\langle \gamma \rangle = \frac{\gamma + |\gamma|}{2} \quad \forall \gamma \in \Re \tag{3}$$

The characteristic length can be computed, according to Bazant and Oh [12], for square elements as:

$$L_c = \frac{\sqrt{A_{ip}}}{\cos\theta} \tag{4}$$

where A_{ip} is the area associated to an element integration point, while θ is the angle between the crack direction and the mesh line where the crack advances.

Table 2. Equivalent displacement and stress definition

Failure mode		δ_{eq}	σ_{eq}
Fiber tension	$\bar{\sigma}_{11} > 0$	$L_c\sqrt{\langle\varepsilon_{11}\rangle^2 + \alpha\cdot\varepsilon_{12}^2}$	$\dfrac{L_c\left(\langle\sigma_{11}\rangle\langle\varepsilon_{11}\rangle + \alpha\cdot\sigma_{12}\cdot\varepsilon_{12}\right)}{\delta_{ft,eq}}$
Fiber Compression	$\bar{\sigma}_{11} < 0$	$L_c\langle-\varepsilon_{11}\rangle$	$\dfrac{L_c\langle-\sigma_{11}\rangle\langle-\varepsilon_{11}\rangle}{\delta_{fc,eq}}$
Matrix tension	$\bar{\sigma}_{22} \geq 0$	$L_c\sqrt{\langle\varepsilon_{22}\rangle^2 + \varepsilon_{12}^2}$	$\dfrac{L_c\left(\langle\sigma_{22}\rangle\langle\varepsilon_{22}\rangle + \sigma_{12}\cdot\varepsilon_{12}\right)}{\delta_{mt,eq}}$
Matrix compression	$\bar{\sigma}_{22} \leq 0$	$L_c\sqrt{\langle-\varepsilon_{22}\rangle^2 + \varepsilon_{12}^2}$	$\dfrac{L_c\left(\langle-\sigma_{22}\rangle\langle-\varepsilon_{22}\rangle + \sigma_{12}\cdot\varepsilon_{12}\right)}{\delta_{mc,eq}}$

3. Model description

The mechanical behaviour of omega reinforced composite panels with large notch damages has been investigated in this work [13,14]. Indeed, the panel has been manufactured by using two laminates *[0/90]*$_s$. The first laminate has been adopted for the panel skin manufacturing, while the second laminate has been used to manufacture the stringers (sse Figure 2 side). As a consequence, the stacking sequence in the bays is *[0/90/90/0]*$_s$.

The geometry of the panel and the boundary conditions are shown in Figure 2. Referring to Figure 2, a compressive displacement has been applied on the **BC** edge, while the **AD** edge has been clamped.

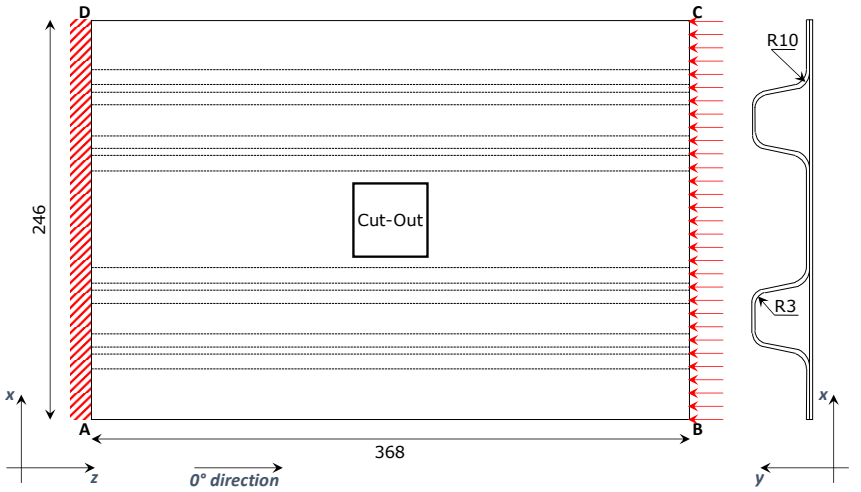

Figure 2: Geometry of the stiffened composite panel (dimensions in *mm*)

A *20 mm* × *4 mm* large notch damage has been considered in the middle of the central bay. The three different damage configurations, shown in Figure 3, have been investigated in this work: a configuration with a notch oriented parallel to the loading direction (Figure 3.a), a configuration with a notch oriented normally to the loading

direction (Figure 3.b) and a configuration with a notch oriented at 45° with respect to the loading direction. (Figure 3.c).

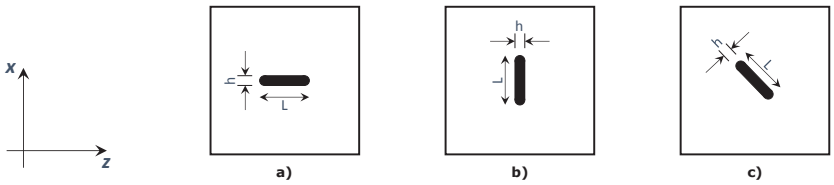

Figure 3: large notch damage region: damage configurations (L = 20 *mm*; h = 4 *mm*)

The lamina properties of the adopted composite material system are presented in Table 3.

Table 3: Material properties

Properties	**Value**
Orthotropic properties	E_{11} = 130 050 MPa; E_{22} = 11 550 MPa $G_{12} = G_{23} = G_{13}$ =6 000 MPa $\upsilon_{12} = \upsilon_{23} = \upsilon_{31}$ = 0.312
Strength	X_T = 1 022 MPa; X_C = 614 MPa; Y_T = 54 MPa; Y_C = 169 MPa; $S_{12} = S_{13}$ = 63 MPa; S_{23} = 28 MPa
In-Plane fracture energies	G^T_{1c} = 11.5kJ/m^2; G^C_{1c} = 4.1 kJ/m^2; G^T_{2c} = 0.35 kJ/m^2; G^C_{2c} = 3.2kJ/m^2
Inter-laminar fracture toughness	G_{Ic} = 0.18 kJ/m^2; G_{IIc} = 0.5 kJ/m^2; G_{IIIc} = 0.5 kJ/m^2

The numerical model has been discretized with continuum shell elements. In Figure 4, the Finite Element model of the panel configuration with a 45° large notch damage and a detail of the large notch damage region FE model are shown as an example.

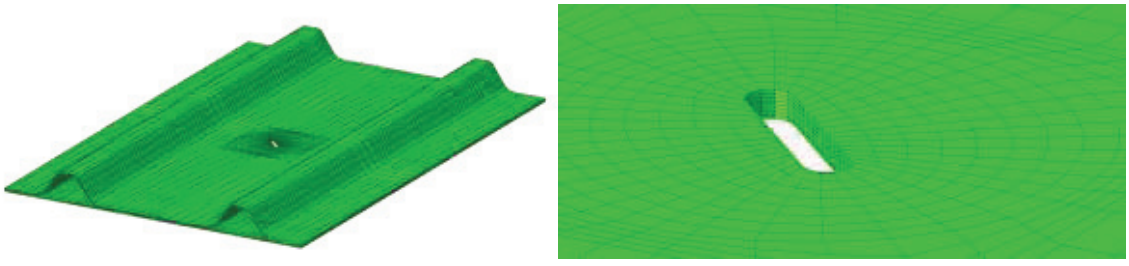

Figure 4: 45° notch damage configuration (Left) Numerical model of the panel; (right) detail of the cut-out region

4. Results

In this section, the numerical results obtained for the three analysed stiffened composite panels configuration are introduced in terms of Load vs. Applied displacements curves and intra-laminar damages extensions.

Indeed, the Load vs. Applied displacements curve shown in Figure 5 demonstrates that a significant variation of the stiffness of the overall structure cannot be observed for the three analysed configurations. However, the maximum load carried by the structure is clearly influenced by the cut-out direction. The analyses have shown that the most critical configuration is the 0° oriented large notch damage, while the configuration with 90° oriented large notch damage seems to be less sensitive to notch. In Table 4, the maximum loads sustainable by the investigated panels are introduced.

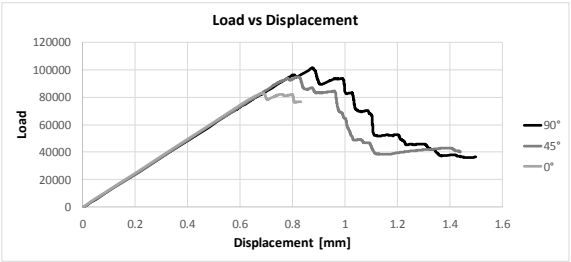

Figure 5: Load vs. Applied displacements for the three analysed configurations

Table 4: Material properties

	0° notch damage	**45° notch damage**	**90° notch damage**
Maximum Load [kN]	*82.84*	*94.87*	*101.46*

The differences in maximum load can be ascribed to the influence of the large notch orientation on the damage behaviour in terms of damage onset and evolution. Such behaviour can be clearly observed in the Figures 6 and Figure 7, where the degradation damage coefficients, related respectively to the Fibre Compression and Matrix Compression Failures, are reported. The damage representations introduced in Figures 6 and Figure 7, obtained for an applied displacement of *0.83 mm,* show that the fibre and matrix damaged areas seems to reach the maximum extension for the 0° large notch configuration. Indeed, for this configuration, from the middle of the bay the fibre and matrix damaged areas extend up to the stringer location.

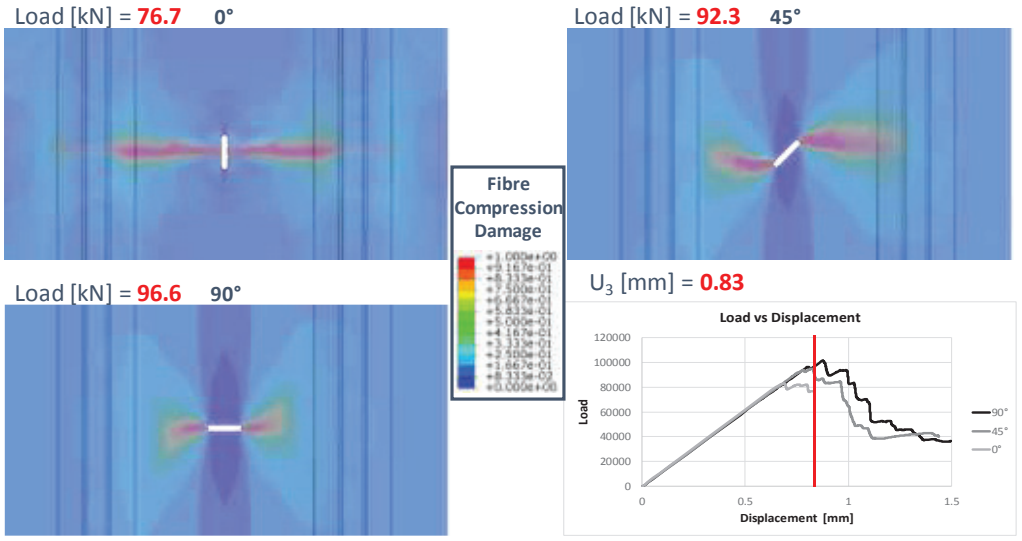

Figure 6: Fibre Compressive degradation damage coefficients for a compressive displacement of 0.83 mm

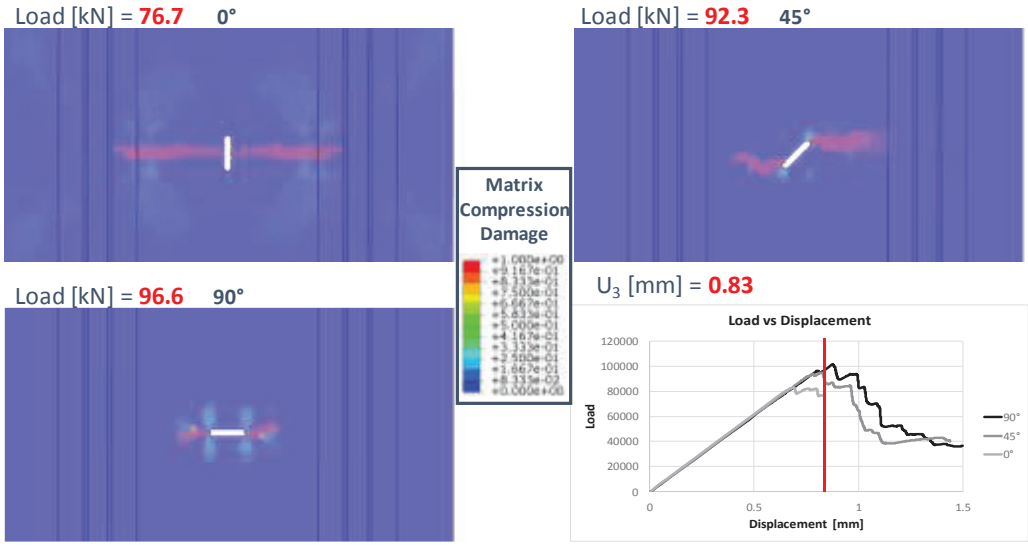

Figure 7: Matrix Compressive degradation damage coefficients for a compressive displacement of 0.83 mm

Finally, Figure 8 focuses on the damages in the large notch region of the 0° configuration. In particular, Figure 8.a, Figure 8.b, Figure 8.c and Figure 8.d show, respectively, the damage accumulation due to fibre compression, fibre tension, matrix compression, and matrix tension failures. According to Figure 8.a, the failure of the fibre in compression affects the 0° oriented laminae, while, according to Figure 8.c, the failure of the matrix in compression affects the 90° oriented laminae. Finally, very small number of elements damaged for fibre tension failure (see Figure 8.b) and for matrix tension failure (see Figure 8.d) can be appreciated in the bottom lamina of the panel probably due to the small out-of-plane displacements observed in the large notch damage region.

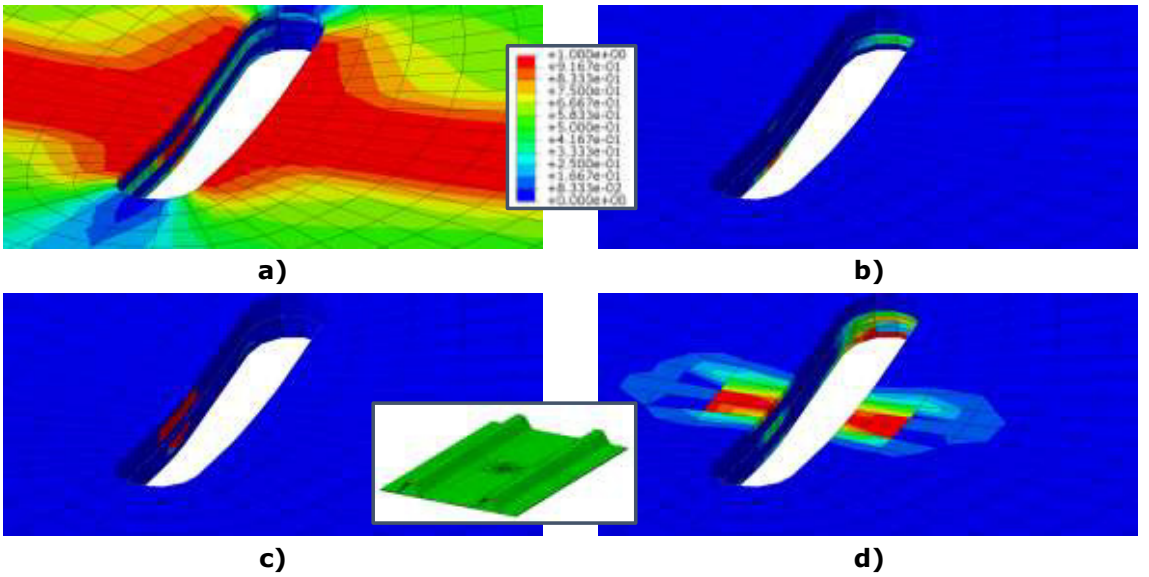

Figure 8: 0° notch damage configuration – degradation damage coefficients for a compressive displacement of 0.83 mm *a)* Fibre compression; *b)* Fibre tension; *c)* Matrix compression; *d)* Matrix tension

5. Conclusions

In this work, the compressive behaviour of large notch damaged stiffened composite panels has been investigated. Three different configurations with differently oriented large notch damages have been studied. Indeed, large notch damages with 0°, 45° and 90° orientation with respect to the applied load direction have been considered.

A Progressive Failure Analysis has been performed on the stiffened composite panels in order to compare the effects of the large notch orientation on their mechanical behaviour including intra-laminar damage evolution.

The results demonstrates that the large notch orientation influences the maximum sustainable load and the damage evolution. In particular, the most critical effects have been found on the configuration with the large notch damage oriented according to the load direction.

Finally, it has been observed, as expected, that the predominant intra-laminar damage failure modes change along the thickness with lamina orientation. Indeed, 0° oriented laminae are the most affected by the fibre failure, while 90° oriented laminae are the most affected by the matrix failure.

References

[1] A. Riccio, A. Raimondo, F. Scaramuzzino, A study on skin delaminations growth in stiffened composite panels by a novel numerical approach. Applied Composite Material 20(4) (2013) 465–488

[2] A. Riccio, F. Scaramuzzino, P. Perugini, Influence of contact phenomena on embedded delaminations growth in composites. AIAA Journal 41(5) (2003) 933–940

[3] R. Borrelli, F. Di Caprio, U. Mercurio, F. Romano, Assessment of progressive failure analysis capabilities of commercial FE codes. International Journal of Structural Integrity 4(3) (2013) 300–320

[4] F. Caputo, A. De Luca, G. Lamanna, V. Lopresto, A. Riccio, Numerical investigation of onset and evolution of LVI damages in Carbon-Epoxy plates. Composites Part B: Engineering 68, 385–391

[5] F. Caputo, A. De Luca, R. Sepe, Numerical study of the structural behaviour of impacted composite laminates subjected to compression load. Composites Part B: Engineering 79, 456–465

[6] F. Romano, F. Di Caprio, B. Auriemma, U. Mercurio, Numerical investigation on the failure phenomena of stiffened composite panels in post-buckling regime with discrete damages. Engineering Failure Analysis 56 (2015) 116–130

[7] R. Borrelli, S. Franchitti, F. Di Caprio, U. Mercurio, A. Zallo, A repair criterion for impacted composite structures based on the prediction of the residual compressive strength. Procedia Engineering 88 (2014) 117–124

[8] D.W. Sleight, Progressive failure analysis methodology for laminated composite structures. Technical Report NASA/TP-1999-209107 (1999)
[9] Z. Hashin, A. Rotem, A Fatigue Criterion for Fiber Reinforced Materials. Journal of Composite Materials 7(4) (1973) 448–464
[10] Z. Hashin, Failure criteria for unidirectional fiber composites. Journal of Applied Mechanics, 47(2) (1980) 329–334
[11] ABAQUS Analysis User's Manual 6.11, 2011
[12] Z.P. Bažant, B.H. Oh, Crack band theory for fracture of concrete. Matériaux et Construction, 16(3) (1983) 155–177
[13] R. Sepe, A. De Luca, G. Lamanna, F. Caputo, Numerical and experimental investigation of residual strength of a LVI damaged CFRP omega stiffened panel with a cut-out. Composites Part B: Engineering 102, 38–56
[14] A. Riccio, S. Saputo, A. Sellitto, A. Raimondo, R. Ricchiuto, Numerical investigation of a stiffened panel subjected to low velocity impacts. Key Engineering Materials 665, 277–280